Inorganic Chemistry Communications 80 (2017) 69–71

Contents lists available at ScienceDirect

Inorganic Chemistry Communications

journal homepage: www.elsevier.com/locate/inoche

Short communication

Strong metal-to-ligand π-backbonding weakens the N—N bond in 2-pyridinealdazine coordinated to tetraammine-ruthenium(II)

Mauricio Cattaneo [a], Pablo Alborés [b], Florencia Fagalde [a], Néstor E. Katz [a,*]

[a] INQUINOA-UNT-CONICET, Instituto de Química Física, Facultad de Bioquímica, Química y Farmacia, Universidad Nacional de Tucumán, Ayacucho 491, T4000INI San Miguel de Tucumán, Argentina
[b] INQUIMAE-UBA-CONICET, DQIAyQF, Universidad de Buenos Aires, Ciudad Universitaria, Pabellón 2, 3°piso, C1428EHA Buenos Aires, Argentina

ARTICLE INFO

Article history:
Received 23 November 2016
Accepted 16 April 2017
Available online 18 April 2017

ABSTRACT

A new mononuclear Ru(II) complex of formula $[Ru(NH_3)_4(2\text{-PCA})](PF_6)_2$, (**1**), with 2-PCA = 2-pyridinealdazine, has been synthesized and characterized by spectroscopic and electrochemical techniques. The complete structure of (**1**) was determined by X-ray diffraction. A strong π-backbonding effect $d_\pi(Ru) \rightarrow \pi^*(2\text{-PCA})$ is disclosed in (**1**) by the high value of the Ru^{III}/Ru^{II} redox potential and the short Ru-N(imine) bond length, which leads to a weakened N—N bond in coordinated 2-PCA compared to that of the free ligand and thus to an enhanced reactivity in acidic media. In effect, the product of the reaction of excess Ru with 2-PCA is not the dinuclear species bridged by 2-PCA, but the already known 2-iminopyridine complex of tetraammineruthenium(II). DFT and TD-DFT calculations of (**1**) were consistent with experimental results and allowed the complete assignment of its UV–Visible bands.

Polypyridyl ligands with the ability to connect two or more metal centers are relevant in designing complex molecular architectures, such as antenna complexes, one-, two-, or tridimensional solids, and systems involved in energy and electron transfer [1]. On the other hand, tetraammineruthenium(II) complexes are important for understanding the influence of π-backbonding effects in electron transfer kinetics and structural parameters of coordination compounds [2].

We have previously reported the synthesis and characterization of dinuclear complexes of formulae: $[(NH_3)_5Ru(\mu\text{-4-PCA})\text{-}Ru(NH_3)_5]^{4+}$ and $[(NH_3)_4Ru(\mu\text{-BBDB})\text{-}Ru(NH_3)_4]^{4+}$, with 4-PCA = 4-pyridinealdazine [3a] and BBDB = 1,4-bis(4-(4′-methyl)-2,2′-bipyridyl)-2,3-diaza-1,3-butadiene) [3b], which displayed considerable electronic coupling between both metal centers, despite their long separation distance. The ligand 2-PCA (2-PCA = 2-pyridinealdazine or 2-pyridinecarboxaldehydeazine or 1,4-bis(2-pyridyl)-2,3-diaza-1,3-butadiene), whose structure is shown in Fig. 1, is similar to the previously mentioned azines, but differs from them in its capacity to coordinate to one or two transition metals by the imine N atoms. Coordination compounds with 2-PCA have already been described [4], but there are no reports on ammineruthenium complexes with this ligand. In this work, we report the synthesis, crystal structure, physicochemical characterization and reactivity of a new species of formula $[Ru(NH_3)_4(2\text{-PCA})](PF_6)_2$, or (**1**).

All used chemicals were reagent grade. CH_3CN was freshly distilled for electrochemical measurements. Tetrakis(*n*-butyl)ammonium hexafluorophosphate (TBAH) was recrystallized four times from EtOH and dried at 150 °C for 72 h. Cyclic voltammetry experiments were carried out in CH_3CN in a BAS Epsilon EC equipment with Ag/AgCl (3 M NaCl) as reference electrode, vitreous C as working electrode, Pt wire as auxiliary electrode and 0.1 M TBAH as supporting electrolyte. Chemical analyses were performed at INQUIMAE (University of Buenos Aires, Argentina), with an estimated error of ±0.5%. IR spectra were performed as KBr pellets on a FTIR Perkin-Elmer RX-I spectrophotometer. UV–Visible spectra were recorded with a Varian Cary-50 spectrophotometer. Emission spectra were obtained with a Shimadzu RF-5301 PC spectrofluorometer at room temperature. NMR were recorded in CD_3CN with a Bruker Avance 200 MHz spectrometer. Spectroelectrochemical measurements in the UV–Visible region were carried out with a Honeycomb Cell from PINE Research Instrumentation.

Computational analysis were carried out with a Gaussian-03 program package [5]. Electronic structure of the ground state of Ru(II) complexes were optimized via density functional theory (DFT). The Becke three parameters hybrid exchange [6a] and the Lee-Yang-Parr correlation functionals (B3LYP) [6b]were used with the LANL2DZ basis set for Ru and 6-311* for C, N and H [7]. The vertical transition energies were calculated at the optimized ground-state geometry for the lowest 50 singlet to singlet excitation energy using time-dependent density functional theory (TD-DFT) with an hybrid B3LYP functional. An approximation to include solvent polarization effects was used by using the CPCM

* Corresponding author.
E-mail address: nkatz@fbqf.unt.edu.ar (N.E. Katz).

http://dx.doi.org/10.1016/j.inoche.2017.04.012
1387-7003/

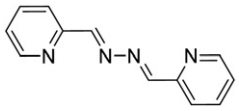

Fig. 1. Structure of 2-PCA.

reaction field model with acetonitrile as a solvent. Mulliken population analysis, partial density of states (PDOS) and simulated electronic spectra were calculated using the GaussSum 3.0 program [8], with a half-width of 5000 cm^{-1}.

To synthetize complex (**1**), a solution of 1 eq of 2-PCA in acetone was bubbled with Ar, under stirring, and covered from light for 30 min. Then, 1 eq of $[Ru(NH_3)_5(H_2O)](PF_6)_2$, prepared as in [9], was added and the reaction was allowed to proceed for 2 h at 50 °C. The original pale yellow solution turned to dark red. Precipitation was induced with 50 mL of $CHCl_3$ and 50 mL of diethyl ether. The obtained solid was filtered, washed with ether, dried, and then chromatographed in alumina with toluene/acetone/methanol 10:5:1. The desired product was evaporated to dryness, re-suspended in acetone, precipitated with diethyl ether, filtered and dried under vacuum over P_4O_{10}. Crystals were obtained by slow evaporation of a concentrated solution of (**1**) in water/acetone 1:1. Several attempts to obtain the dinuclear complex by reacting 2-PCA with 2 eq. of $[Ru(NH_3)_5(H_2O)](PF_6)_2$ at different conditions, times and temperatures, even starting from precursor $[Ru^{III}(NH_3)_4(Cl)_2]Cl$ [10], were unsuccessful. Some reactions in acidic media produce the already described mononuclear complex $[Ru(NH_3)_5(2\text{-impy})](PF_6)_2$, (**2**), with 2-impy = 2-iminopyridine [11].

Anal. % found (calculated) for (**1**)·H_2O or $C_{12}H_{24}F_{12}N_8P_2ORu$: C, 21.1 (21.0); H, 3.2 (3.5); N, 15.6 (16.3). IR (KBr pellets): 3374, 3300, 2970, 2930, 1628, 1467, 1438, 1299, 1278, 1247, 1227, 1161, 1097, 1052, 1024, 998, 850, 779, 762, 741, 558 cm^{-1}. UV–Visible (CH_3CN), λ_{max}, nm (ε_{max}, M^{-1} cm^{-1}): 508 (4.7×10^3), 369 (4.9×10^3), 288 (19.0×10^3), 241 (13.8×10^3). ^1H NMR (CD_3CN), 8.87 (H_1, ddd, 1H, J_{12} = 5.8 Hz, J_{13} = 1.3 Hz, J_{14} = 1 Hz), 7.52 (H_2, ddd, 1H; J_{23} = 7.4, J_{24} = 1.6 Hz), 7.85 (H_3, ddd, 1H; J_{34} = 7.8 Hz), 7.98 (H_4, ddd, 1H), 8.90 (H_6, s, 1H), 8.51 (H_7, s, 1H), 8.24 (H_9, ddd, 1H, J_{910} = 7.9 Hz, J_{911} = 1,2 Hz, J_{912} = 0.9 Hz), 8.03 (H_{10}, ddd, 1H; J_{1011} = 7.5, J_{1012} = 1.7 Hz), 7.59 (H_{11}, ddd, 1H; J_{1112} = 4.8 Hz), 8.78 (H_{12}, ddd, 1H), 3.19 (NH_3, s, 3H), 2.57 (NH_3, s, 3H), 1.49 (NH_3, s, 6H). ^{13}C NMR (CD_3CN), C_1 = 154.14, C_2 = 125.43, C_3 = 135.14, C_4 = 138.23, C_5 = 161.36, C_6 = 155.06, C_7 = 160.08, C_8 = 152.55, C_9 = 123.42, C_{10} = 127.64, C_{11} = 127.15, C_{12} = 151.19 ppm. Numbering of the atoms is displayed in Fig. 2.

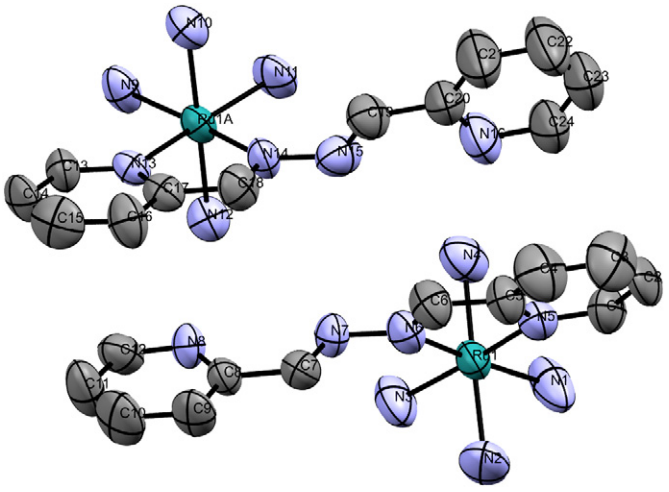

Fig. 2. ORTEP diagrams for two cations of complex (**1**) in the unit cell, with C atoms in black, N atoms in blue and Ru atoms in green. H atoms have been omitted for clarity. (For interpretation of the references to color in this figure legend, the reader is referred to the web version of this article.)

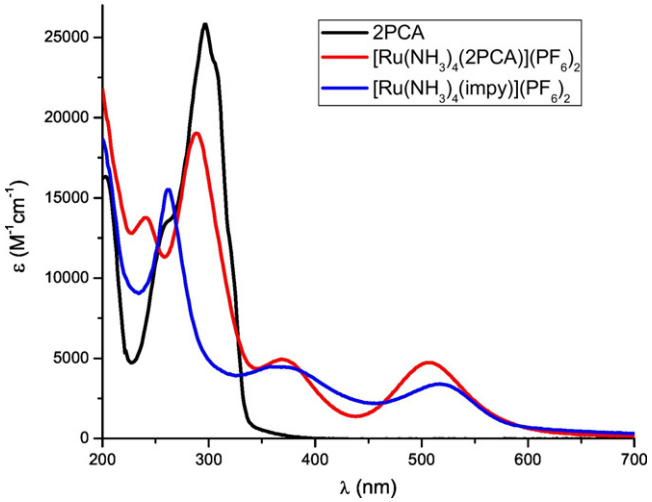

Fig. 3. UV–Visible spectra for 2-PCA and complexes (**1**) and (**2**) in CH_3CN.

Fig. 2 shows an ORTEP diagram of two crystallographic forms of cations of (**1**) in the unit cell, as determined by X-ray diffraction techniques, described in Supplementary information (that includes crystal data in Table S1 and selected bond angles and distances in Table S2). A distorted structure for the ligand 2-PCA is revealed, with dihedral angles —C═N—N═C— of 61(1) and 71(1)° for both forms. Low rotational energy allows this conformation for the ligand [12]. The reported N—N distance in uncoordinated 2-PCA is 1.413(1) Å [13], while for both crystallographic forms of this complex, values of 1.43(1) and 1.44(1) Å are determined, indicating weakening of the N—N bond order due to strong π-backbonding from Ru(II) to the imine Ns, a fact reflected in the short Ru-N(imine) bond lengths for both forms: 1.995(9) and 1.963(8) Å, values which can be compared to the usual Ru—N distances in polypyridyl complexes (1.97–2.09 Å) [14]. Besides, considerable π-π stacking of the pyridyl rings of 2-PCA and hydrogen bonds between Hs of the NH_3 groups and the uncoordinated Ns of the pyridyl groups of both forms are also disclosed. These interactions contribute to the short distance between both cations.

Electronic absorption of (**1**) is very similar to other structurally analogous complexes, such as (**2**) and $[Ru(NH_3)_4(bpy)]^{2+}$ (bpy = 2,2′-bipyridine) [11,15]. They all display two MLCT bands between 500

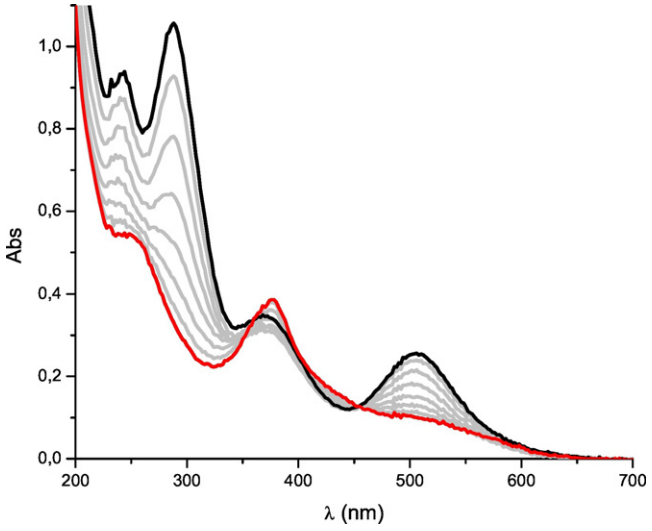

Fig. 4. UV–Visible Spectroelectrochemistry for **(1)** at 900 mV in CH_3CN, 0.1 M TBAH, going from the black line (t = 0) to the red line (t = 10 min). (For interpretation of the references to color in this figure legend, the reader is referred to the web version of this article.)

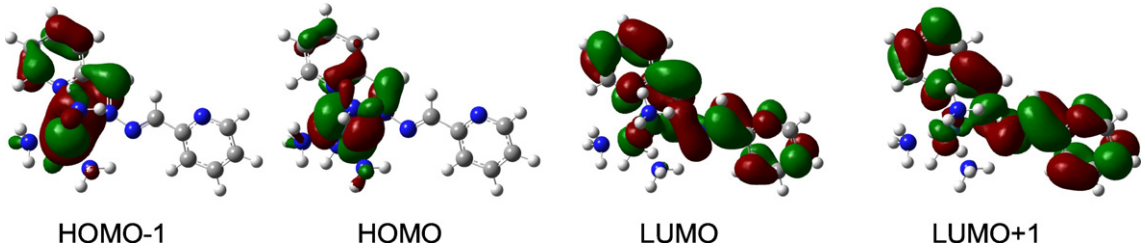

Fig. 5. Frontier molecular orbitals of complex (**1**).

and 520 nm and 350–400 nm and intraligand π-π* absorptions below 300 nm. For comparison purposes, UV–Visible spectra of free 2-PCA and complexes (**1**) and (**2**) are shown in Fig. 3.

Electrochemical measurements of (**1**) by cyclic voltammetry shows a reversible voltammetric wave corresponding to the Ru(III)/Ru(II) couple at $E_{1/2} = 0.79$ V (vs. Ag/AgCl), a value considerably higher than that corresponding to complex (**2**) ($E_{1/2} = 0.63$ V, vs. Ag/AgCl). This result indicates enhanced π-backbonding from Ru(II) to 2-PCA, as compared to π-backbonding from Ru(II) to 2-impy, possibly due to higher electronic delocalization in 2-PCA.

UV–Visible spectroelectrochemistry of (**1**) to form the Ru^{III} species is shown in Fig. 4. Depletion of MLCT transitions and rising of LMCT transitions at slightly lower energies are observed with some decomposition, as disclosed by depletion of the IL band.

NMR spectra are shown in Supplementary information as Fig. S1–S4. 2-PCA has C_{2h} symmetry, which gives rise to a set of 5 signals that integrate for 2 protons each in the ^{1}H NMR spectrum. Coordination of 2-PCA to Ru (**1**) disrupts the symmetry of the ligand, originating a set of 10 signals, while the set of 5 signals remains in complex (**2**). Protons of the coordinated part of 2-PCA are deshielded respect to the free ligand. Besides, four N signals are detected in its ^{15}N NMR spectrum in CD_3CN, with two values similar to the imine and pyridine nitrogens of the free ligand (365 and 317 ppm) and two corresponding to the imine and pyridine nitrogens coordinated to the metal (335 and 251 ppm).

Computational analysis were carried out in (**1**) and (**2**), and are shown in Fig. S5 and Table S3 of Supplementary information. The results are consistent with those found experimentally. TD-DFT calculations (Table S4) reproduced UV–visible spectra for both complexes (Fig. S6), with the lowest energy bands being assigned to MLCT transitions from d_π(Ru) HOMO − 1 to LUMO (centered in the imine group of the azine ligands) orbitals. The bands at higher energies in the visible region are assigned to MLCT transitions from d_π(Ru) HOMO − 1 to LUMO + 1 (centered in the pyridine moiety of the azine ligands). Fig. 5 shows a GaussView diagram of the frontier MOs of (**1**). The HOMOs – being mostly d_{xy} in character – do not overlap with π* orbitals of the azines. These theoretical assignments of the visible bands are in complete agreement with experimental evidence found previously in similar species [11]. Due to the presence of two pyridyl rings in 2-PCA, electronic delocalization in (**1**) is expected to be higher than in (**2**), supporting the considerable metal-to-ligand π-backbonding effect d_π(Ru) → π*(2-PCA) that was found experimentally.

To conclude, we have prepared the first complex of 2-PCA with a tetraammineruthenium(II) group. The structural, spectroscopic and computational data of this new species put into evidence a strong π-backbonding effect from Ru(II) to the imine N of 2-PCA. As a consequence, the N—N bond is weakened and its reactivity is increased. In slightly acidic media, the N—N bond is cleaved, giving rise to the 2-iminopyridine complex and thus avoiding the formation of a dinuclear symmetrical complex of two tetraammineruthenium moieties bridged by 2-PCA. However, complex (**1**) might be used as structural block for preparing new asymmetrical dinuclear complexes for modeling intramolecular electron transfer processes.

Acknowledgments

We thank Universidad Nacional de Tucumán (UNT) (PIUNT2014-D/547), Consejo Nacional de Investigaciones Científicas y Técnicas (CONICET) (PIP2015-098), and Agencia Nacional de Promoción Científica y Tecnológica (ANPCyT) (PICT2011-1553), all from Argentina, for financial support. M.C., P. A., F.F. and N.E.K. are Members of the Research Career from CONICET, Argentina.

Appendix A. Supplementary data

Supplementary data to this article can be found online at http://dx.doi.org/10.1016/j.inoche.2017.04.012.

References

[1] J.L. Boyer, J. Rochford, M. Tsai, J.T. Muckerman, E. Fujita, Coord. Chem. Rev. 254 (2010) 309.
[2] P.C. Ford, Coord. Chem. Rev. 5 (1970) 75.
[3] a) M. Cattaneo, F. Fagalde, N.E. Katz, A.M. Leiva, R. Schmehl, Inorg. Chem. 45 (2006) 127;
b) M. Cattaneo, M.M. Vergara, M.E. García Posse, F. Fagalde, T. Parella, N.E. Katz, Polyhedron 70 (2014) 20.
[4] a) W.J. Stratton, M.F. Rettig, R.F. Drury, Inorg. Chim. Acta 3 (1969) 97;
b) M.M. Dawod, F.I. Khalili, A.M. Seyam, Polyhedron 8 (1989) 218;
c) X.-H. Zhou, T. Wu, D. Li, Inorg. Chim. Acta 359 (2006) 1442;
d) M. Haga, K. Koizumi, Inorg. Chim. Acta 104 (1985) 47;
e) S. Chakraborty, P. Munshi, G.K. Lahiri, Polyhedron 18 (1999) 1437;
f) N.M. Shavaleev, Z.R. Bell, G. Accorsi, M.D. Ward, Inorg. Chim. Acta 351 (2003) 159.
[5] M.J. Frisch, et al., Gaussian-03, Revision C.02, Gaussian, Inc., Wallinford, CT, 2004.
[6] a) A.D. Becke, J. Chem. Phys. 98 (1993) 5648;
b) C. Lee, W. Yang, R.G. Parr, Phys. Rev. B 37 (1988) 785.
[7] a) L. Yang, A.-M. Ren, J.-K. Feng, X.-D. Liu, Y.-G. Ma, H.-X. Zhang, Inorg. Chem. 43 (2004) 5961;
b) L. Yang, A.-M. Ren, J.-K. Feng, X.-D. Liu, Y.-G. Ma, M. Zhang, J.-C. Shen, H.-X. Zhang, J. Phys. Chem. A 108 (2004) 6797.
[8] N.M. O'Boyle, A.L. Tenderholt, K.M. Langner, J. Comput. Chem. 29 (2008) 839.
[9] J.E. Sutton, H. Taube, Inorg. Chem. 20 (1981) 3125.
[10] S.E. Boggs, R.E. Clarke, P.C. Ford, Inorg. Chim. Acta 247 (1996) 129.
[11] V.E. Alvarez, R.J. Allen, T. Matsubara, P.C. Ford, J. Am. Chem. Soc. 96 (1974) 7686.
[12] S.K. Singh, M. Chandra, D.S. Pandey, M.C. Puerta, P. Valerga, J. Organomet. Chem. 689 (2004) 3612.
[13] E.C. Kesslen, W.B. Euler, B.M. Foxman, Chem. Mater. 11 (1999) 336.
[14] G. Pourrieux, F. Fagalde, N.E. Katz, T. Parella, J. Benet-Buchholz, A. Llobet, Polyhedron 27 (2008) 2990.
[15] J.C. Curtis, B.P. Sullivan, T.J. Meyer, Inorg. Chem. 22 (1983) 224.